Exploring the origins of binding specificity through the computational redesign of calmodulin

Julia M. Shifman and Stephen L. Mayo*

Howard Hughes Medical Institute and Division of Biology, California Institute of Technology, Mail Code 114-96, Pasadena, CA 91125

Calmodulin (CaM) is a second messenger protein that has evolved to bind tightly to a variety of targets and, as such, exhibits low binding specificity. We redesigned CaM by using a computational protein design algorithm to improve its binding specificity for one of its targets, smooth muscle myosin light chain kinase (smMLCK). Residues in or near the CaM/smMLCK binding interface were optimized; CaM interactions with alternative targets were not directly considered in the optimization. The predicted CaM sequences were constructed and tested for binding to a set of eight targets including smMLCK. The best CaM variant, obtained from a calculation that emphasized intermolecular interactions, showed up to a 155-fold increase in binding specificity. The increase in binding specificity was not due to improved binding to smMLCK, but due to decreased binding to the alternative targets. This finding is consistent with the fact that the sequence of wild-type CaM is nearly optimal for interactions with numerous targets.

Identifying the interactions responsible for conveying binding specificity in proteins is critical to understanding protein function and is a prerequisite for the design of novel protein receptors and ligands. Here, we explore the basis of binding specificity in calmodulin (CaM). CaM is a ubiquitous Ca^{2+}-binding protein that binds to and regulates a variety of proteins (1–5). Numerous biochemical studies on CaM (6–9), as well as several x-ray and NMR structures of CaM-target complexes (10–17), have revealed many aspects of the target recognition mechanism in this molecule. CaM usually interacts with proteins by binding to stretches of 14- to 30-aa residues capable of forming amphipathic α-helices. Although specific interactions between CaM and its targets differ depending on the target identity, the general topology of CaM-target complexes remains the same (Fig. 1). On binding, CaM embraces its targets with its C- and N-terminal globular domains, inducing a coil–to–helix transition in the target (18).

CaM has evolved to bind to multiple targets with equally high affinity and, as such, exhibits low binding specificity. To explore the nature of the interactions conferring (the lack of) binding specificity in CaM, we redesigned CaM so it would favor binding to one of its natural targets, smooth muscle myosin light chain kinase (smMLCK). Starting from the crystal structure of the CaM–smMLCK complex (11), we optimized the CaM-binding interface by using ORBIT (optimization of rotamers by iterative techniques), a program that has been successfully applied to protein design and stabilization (19–23). In previous work, we demonstrated that the binding specificity of CaM could be improved by redesigning a number of core positions in the CaM-binding interface (24). The designed 8-fold CaM variant, CaM_core (designated CaM_8 in previous work), exhibited binding affinity for the desired target that was similar to wild type and showed an increase in binding specificity of up to 120-fold.

In this study, we sought to increase CaM-binding specificity further by extending the optimization to boundary and surface positions in the CaM–smMLCK-binding interface. These positions, occupied mostly by glutamates, are likely to play a major role in the CaM target recognition mechanism because of the positively charged nature of the target sequences. Initially, we used computational protein design methods that were developed for stabilization of single proteins (25). However, when these methods yielded poor results, we refined the computational procedure for optimization of protein–target complexes by exploring the use of a modified energy function as well as different optimization parameters. Finally, we discuss the importance of including negative design when optimizing protein interfaces for improved binding specificity.

Materials and Methods

Computational Methods. All residues in the CaM–smMLCK crystal structure (11) were divided into core, boundary, and surface classes as described (19). Eight CaM surface and boundary positions (positions 14, 83, 87, 114, 116, 120, 123, and 127) that are within 4 Å of smMLCK were selected for optimization. The following amino acids were allowed at each of the optimized positions: Ala, Val, Leu, Ile, Met, Phe, Tyr, Trp, Ser, Thr, Asp, Asn, His, Glu, Gln, Lys, and Arg. The identities of the core residues in the CaM–smMLCK interface were set to those of a previously designed CaM variant, CaM_core (designated CaM_8 in previous work; ref. 24). The side chain conformations of the core residues, as well as those of the smMLCK residues, were allowed to change during the optimization. The designed sequences were obtained by using either previously described procedures (24) (CaM_core and CaM_boundary) or by using the variations described in the main text (CaMmod$_{boundary}^{no\_bias}$ and CaMmod$_{boundary}^{bias}$). Rotamer libraries used for the CaM optimizations were based on the backbone dependent library of Dunbrack and Karplus (26). A potential energy function that included terms for van der Waals, electrostatic, and hydrogen bonding interactions, and surface area-based solvation was used to calculate side chain/side chain and side chain/backbone pairwise interactions as described (19, 25, 27). The calculated energies served as input to a side-chain selection procedure that used either the Dead-End Elimination theorem (28, 29) (CaM_core and CaM_boundary) or a Monte Carlo algorithm (30, 31) (CaMmod$_{boundary}^{no\_bias}$ and CaMmod$_{boundary}^{bias}$). All CaM optimizations were performed by using SGI R10000 processors (Silicon Graphics, Mountain View, CA) running at 195 MHz.

Protein Expression. CaM variant genes were constructed by using a recursive PCR procedure (32) with six primers. Wild-type and mutant CaM genes were cloned into pET-11 (Novagen) and expressed by isopropyl β-D-thiogalactoside (IPTG) induction in BL21(DE3) hosts (Invitrogen). Proteins were purified by reverse-phase HPLC with a water/acetonitrile gradient containing 0.1% trifluoroacetic acid, lyophilized, and stored at −20°C. Protein masses were verified by electrospray mass spectroscopy.

Peptide Synthesis. Seven peptides, corresponding to CaM-binding domains in target proteins, were selected to assess binding to the CaM variants: smMLCK (-ARRKWQKTGHAVRAIGRLSS-); skMLCK (-KRRWKKNFIAVSAANRFKKISSSGA-); melittin
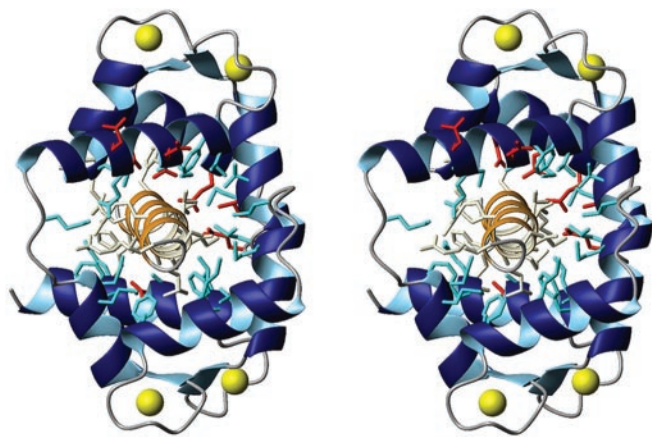
Fig. 1. X-ray structure of CaM in complex with smMLCK (PDB code 1CDM) generated with MOLMOL (40). Ca^{2+} atoms are shown as yellow spheres. The CaM surface and boundary residues selected for optimization are shown in red. The core residues in the CaM-binding interface, shown in cyan, and the smMLCK residues, shown in light yellow, were allowed to change conformation during the optimization procedure. The identities of the CaM core residues were fixed to those of CaM_{core}, a core-optimized CaM variant.

(-QQRKRKIWSILAPLGTTLVKLVAGIG-); spectrin (-KTA-SPWKSARLMVHTVATFNSIKE-); CaMKI (-AKSKWKQAF-NATAVVRHMRKLQ-); CaMKII (-LKKFNARRKLKGAIL-TTMLATRNFS-); and CaMKK (-RFPNGFRKRHGMA-KVLILTDLRPIRRV-). The eighth target, peptide 1 (-LKWKKL-LKLLKKLLKLG-), was designed to bind CaM (33). The peptide targets were synthesized and purified as described (24).

Binding Experiments. Binding of the Trp-containing CaM targets (smMLCK, skMLCK, melittin, peptide 1, CaMKI, and spectrin) was measured by fluorescence spectroscopy, and binding of fluorescently silent targets (CaMKII and CaMKK) to CaM was assessed by circular dichroism spectroscopy as described (24).

Results and Discussion

Boundary and Surface Optimization with Standard Methods. Eight boundary and surface positions within 4 Å of the smMLCK peptide in the CaM–smMLCK structure (11) were selected for the optimization (Fig. 1). In addition, the 24 CaM core residues in the CaM-binding interface were allowed to change conformation, but their amino acid identities were fixed to those of CaM_{core}, a previously optimized CaM core variant that showed improved binding specificity for smMLCK (24). All of the smMLCK residues were allowed to change conformation. For the first CaM boundary and surface optimization, previously published computational protein design methods were used. The optimization produced $CaM_{boundary}$, a protein with 6 boundary and surface substitutions in addition to the 8 mutations of

CaM_{core}, for a total of 14 mutations with respect to wild-type CaM (CaM_{wt}) (Table 1). $CaM_{boundary}$ was expressed, purified, and tested for binding to smMLCK by using fluorescence spectroscopy as described (24). The binding affinity (K_d) was determined to be 114 ± 80 nM. This value is substantially worse than the binding affinities observed for CaM_{wt} and CaM_{core} (1.8 ± 1.3 and 1.3 ± 0.9 nM, respectively).

To determine the source of $CaM_{boundary}$'s decreased affinity for smMLCK, six additional CaM variants were constructed, each with a single boundary or surface substitution from the $CaM_{boundary}$ design in addition to the eight core mutations of CaM_{core}. Titrations of these variants with smMLCK revealed that the decrease in $CaM_{boundary}$'s affinity to smMLCK was largely due to a single mutation, E87L. This mutation produced a CaM_{core} variant, CaM_{core}E87L, with a binding affinity of 50 ± 8 nM. CaM_{core}E127Q had a significant but less deleterious effect on binding, giving a binding affinity of 8.2 ± 2.8 nM. The remaining four CaM_{core} mutants (CaM_{core}E14D, CaM_{core}E83R, CaM_{core}E114I, and CaM_{core}L116E) showed no decrease in binding to smMLCK compared with CaM_{wt} and CaM_{core}.

Analysis of the Standard Computational Methods. The failure of $CaM_{boundary}$ to retain tight binding to smMLCK highlighted the inability of the basic design methods to predict favorable intermolecular interactions. This result was not surprising because the methods were developed for stabilization of isolated proteins rather than protein–protein interfaces. A similar observation was recently made for the use of protein folding-optimized potential functions for describing protein–protein interfaces. These potentials work well when applied to hydrophobic binding interfaces (equivalent to the CaM_{core} design) but fail for hydrophilic interfaces (equivalent to the $CaM_{boundary}$ design) (34). Examination of the interactions predicted in the $CaM_{boundary}$–smMLCK complex revealed several possible problems with the computational methods.

In the CaM optimization, all of the molecular interactions were treated equally whether they were within CaM or between CaM and smMLCK. Such an approach is likely to produce CaM sequences with improved intramolecular interactions at the expense of eliminating favorable CaM–smMLCK intermolecular interactions, which are clearly important for binding. To address this problem, we modified the existing energy function, biasing it toward selection of more favorable intermolecular interactions. A parameter β was introduced into the pairwise portion of the energy function to enhance the intermolecular side chain/side chain interactions and to attenuate the intramolecular side chain/side chain interactions:

$$
\begin{aligned}
E_{\text{CaM–t}}^{\text{bias}} &= \beta E_{\text{CaM–t}}^{\text{nobias}} \\
E_{\text{CaM–CaM}}^{\text{bias}} &= (2 - \beta) E_{\text{CaM–CaM}}^{\text{nobias}} \\
E_{\text{t–t}}^{\text{bias}} &= (2 - \beta) E_{\text{t–t}}^{\text{nobias}}
\end{aligned}
\qquad [1]
$$

Table 1. Binding of boundary- and surface-optimized CaM variants to smMLCK

	Designed positions*															K_d, nM
	11	12	14	55	76	83	84	87	91	109	114	116	120	123	127	145	
CaM_{wt}	E	F	E	V	M	E	E	E	V	M	E	L	E	E	E	M	1.8 ± 1.3
CaM_{core}	**L**	**Y**	—	**I**	**E**	—	**Y**	—	**I**	**L**	—	—	—	—	—	**I**	1.3 ± 0.9
$CaM_{boundary}$	**L**	**Y**	D	**I**	**E**	R	**Y**	L	**I**	**L**	I	E	—	—	Q	**I**	114 ± 83
$CaMmod_{boundary}^{no\text{-}bias}$	**L**	**Y**	—	**I**	**E**	R	**Y**	K	**I**	**L**	I	E	—	K	—	**I**	6.1 ± 0.8
$CaMmod_{boundary}^{bias}$	**L**	**Y**	—	**I**	**E**	R	**Y**	K	**I**	**L**	I	E	—	Q	—	**I**	2.3 ± 0.7

*Eight boundary and surface positions in the CaM–smMLCK binding interface were optimized. Dashes indicate sequence identity to CaM_{wt}. Eight core mutations, shown in bold, were carried over from CaM_{core}.
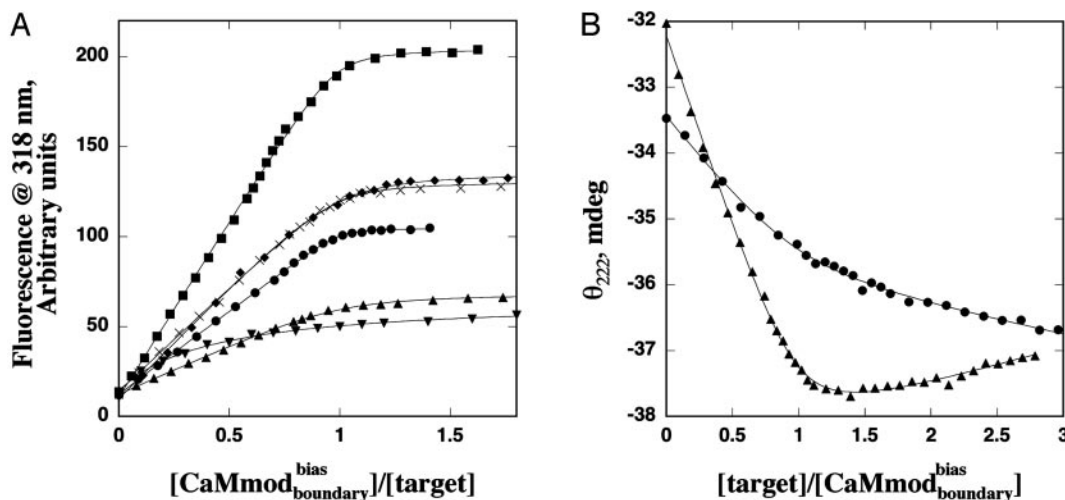
Fig. 2. CaMmod$_{boundary}^{bias}$ binding to target peptides. (*A*) Titration curves corresponding to binding of the Trp containing targets to CaMmod$_{boundary}^{bias}$ monitored by fluorescence at 318 nm: smMLCK (●), skMLCK (♦), spectrin (×), peptide 1 (▼), melittin (▲), and CaMKI (■). (*B*) Titration curves corresponding to binding of CaMmod$_{boundary}^{bias}$ to the fluorescently silent targets monitored by circular dichroism: CaMKK (●) and CaMKII (▲).

Here, E_{CaM-t}^{bias}, $E_{CaM-CaM}^{bias}$, and E_{t-t}^{bias} denote the modified energy functions for the interactions between CaM and the target, within CaM, and within the target, respectively. E_{CaM-t}^{nobias} describes the unbiased intermolecular interactions between CaM and the target; $E_{CaM-CaM}^{nobias}$ and E_{t-t}^{nobias} describe the unbiased intramolecular interactions within CaM and the target, respectively. The optimal value of the parameter β was estimated to be in the 1.2–1.6 range, which was determined by performing a number of CaM–smMLCK optimizations and by visually inspecting the computational results.

An additional concern was the large distance-dependent dielectric constant ($\varepsilon = 40r$) used in the calculation. Although historically satisfactory, the use of a large dielectric constant effectively underemphasized the long-range electrostatics term in the energy function relative to more local terms such as van der Waals and hydrogen bonding interactions. Electrostatic interactions, however, are likely to play a key role in the CaM target recognition mechanism. Their importance is supported by the presence of many negatively charged residues in the CaM-binding interface and the positively charged nature of all known CaM target sequences. Hence, lowering the dielectric constant in the CaM boundary- and surface-optimization might help to restore high binding affinity to smMLCK for the variants generated. A dielectric constant of $4r$ was selected because this value was found to be optimal for the design of β-sheet surface residues (35) and it is in the range of values generally used for calculations of protein binding free energies (36–38).

The small size of the rotamer library used in the calculation is also a concern. To reduce computational time, we selected a rotamer library similar to the one used in previous protein design calculations. In this library, no expansion about the χ_1 and χ_2 side chain dihedral angles was performed for polar residues, resulting in a relatively small number of rotamers for the polar amino acids. However, polar residues are thought to be especially important for CaM target binding. The absence of appropriate side chain rotamers could have resulted in selection of CaM sequences with suboptimal interactions with smMLCK. To reduce this concern, a rotamer library that contained rotamers representing expansion about both χ_1 and χ_2 for all amino acids was used as an option in subsequent calculations.

Redesign of the CaM–smMLCK-Binding Interface Using Modified Methods. Six additional CaM optimizations were performed with and without biasing of the energy function, by using dielectric

constants of $4r$ or $40r$, and the standard or large rotamer libraries (see Table 4, which is published as supporting information on the PNAS web site). Starting from the minimum-energy solution obtained for the CaM core optimization, CaM$_{core}$, a Monte Carlo search algorithm (30, 31) was used to optimize the eight boundary and surface residues in the CaM–smMLCK-binding interface. A Monte Carlo search algorithm was used (instead of the dead-end elimination method) to rapidly explore different computational protocols. Computationally predicted CaM variants were then constructed, and their binding affinities to smMLCK were determined.

Two of six tested variants showed good binding to smMLCK. Both variants were predicted by using a dielectric constant of $4r$ and the large rotamer library. The first variant, CaMmod$_{boundary}^{no\_bias}$, was obtained without introducing biasing into the energy function; the second variant, CaMmod$_{boundary}^{bias}$, was obtained by using the biased energy function (Table 1). CaMmod$_{boundary}^{no\_bias}$ bound to smMLCK almost as well as CaM$_{wt}$ and CaM$_{core}$, showing a K_d value of 6.1 $\pm$ 0.8 nM (Table 1). CaMmod$_{boundary}^{bias}$ performed even better, exhibiting a binding affinity of 2.3 $\pm$ 0.7 nM, similar to that of CaM$_{wt}$. Analysis of the computational methods and binding data for all of the variants (see Table 4) suggests that reducing the dielectric constant to $4r$ and increasing the rotamer library size have a roughly equal effect on improving binding affinity, with each modification improving binding by about a factor of 4.5. Biasing the energy function to emphasize intermolecular interactions provides an additional factor of 2.7 in binding affinity. Combining the three modifications gives the maximal improvement. CaMmod$_{boundary}^{bias}$ was selected for further analysis.

Binding Specificity of CaMmod$_{boundary}^{bias}$. To determine the binding specificity of CaMmod$_{boundary}^{bias}$, we assessed its binding to a set of seven alternative targets; these targets were not included in the model used for the CaM optimization calculations. Binding of CaMmod$_{boundary}^{bias}$ to the Trp-containing targets (skMLCK, spectrin, melittin, peptide 1, and CaMKI) was assessed by fluorescence spectroscopy; binding of CaMmod$_{boundary}^{bias}$ to the fluorescently silent targets (CaMKII and CaMKK) was monitored by circular dichroism spectroscopy. Fig. 2 *A* and *B* shows the titration curves for CaMmod$_{boundary}^{bias}$ binding to the selected targets. CaM$_{wt}$ binds to seven of eight targets equally well, with dissociation constants in the low nM range; weaker binding (K_d

Table 2. Binding affinities (K_d, nM) of WT and redesigned CaM to selected targets

	smMLCK	skMLCK	Spectrin	Melittin	Peptide1	CaMKI	CaMKII	CaMKK
CaM$_{wt}$	1.8 ± 1.3	3.3 ± 0.8	3.3 ± 1.5	28 ± 5	1.7 ± 0.8	1.7 ± 0.7	5.1 ± 1.5	1.0 ± 3.0
CaM$_{core}$	1.3 ± 0.9	4.9 ± 1.2	16 ± 6.0	54 ± 18	147 ± 48	1.3 ± 0.8	54 ± 20	32 ± 13
Decrease in binding*	0.72	1.5	4.8	1.9	86	0.76	11	32
Specificity increase†	1.0	2.1	6.7	2.6	120	1.1	15	44
CaMmod$_{boundary}^{bias}$	2.3 ± 0.7	21 ± 3	11 ± 2	33 ± 6	343 ± 66	7 ± 2	27 ± 6	67 ± 28
Decrease in binding*	1.3	6.4	3.3	1.2	202	4.1	5.3	67
Specificity increase†	1.0	4.9	2.6	0.9	155	3.2	4.1	51

*Decrease in binding was calculated by taking the ratio of binding affinities of a CaM variant and CaM$_{wt}$ for a particular target.
†Specificity increase was calculated by taking the ratio of binding affinity of a CaM variant and CaM$_{wt}$ for a particular target and dividing it by the same ratio for smMLCK.

of 28 ± 5 nM) is observed for melittin (Table 2). Binding of CaMmod$_{boundary}^{bias}$ to all of the alternative targets except melittin was reduced with respect to CaM$_{wt}$. Melittin exhibited similar binding affinities for CaMmod$_{boundary}^{bias}$ and CaM$_{wt}$. Furthermore, binding of CaMmod$_{boundary}^{bias}$ to four of seven of the alternative targets was lowered in comparison to CaM$_{core}$. When compared with CaM$_{core}$, CaMmod$_{boundary}^{bias}$ showed similar binding to spectrin, melittin, and CaMKII, and reduced binding to skMLCK, peptide 1, CaMKI, and CaMKK. The greatest loss (200-fold) in binding affinity to CaMmod$_{boundary}^{bias}$ is observed for peptide 1, which contains a nonnatural target sequence that was engineered to bind CaM without considering specific CaM-target interactions (33). Particularly noteworthy is the ability of CaMmod$_{boundary}^{bias}$ to discriminate against the skMLCK peptide. Unlike CaM$_{core}$, which showed little decrease in binding to skMLCK, CaMmod$_{boundary}^{bias}$ exhibits a 6-fold decrease in binding to this target when compared with CaM$_{wt}$. The sequence of skMLCK is very similar to that of smMLCK, and, hence, these peptides would be expected to present very similar binding surfaces, making it difficult to discriminate between them. Overall, CaMmod$_{boundary}^{bias}$ showed increased binding specificity compared with CaM$_{wt}$ and CaM$_{core}$. CaMmod$_{boundary}^{bias}$ retained the tight binding affinity of CaM$_{wt}$ for the desired target and exhibited a up to 200-fold decrease in binding to the alternative targets (Table 2).

Analysis of the Interactions Predicted in the Redesigned CaM–smMLCK Complexes. Six mutations that distinguish CaM$_{boundary}$ from CaM$_{core}$ produced almost a 100-fold decrease in binding to the desired target, smMLCK (Table 1). Among these mutations, only two had a substantial effect on binding. The E87L mutation was identified as causing the majority of the decrease in binding

affinity. This result was unexpected because Glu-87 does not interact with the target in the CaM$_{wt}$–smMLCK complex. Rather, it forms an intramolecular salt bridge to Arg-90, the disruption of which in CaMmod$_{boundary}^{no\_bias}$ and CaMmod$_{boundary}^{bias}$ does not diminish binding. It is possible that the E87L mutation reduced binding by decreasing the overall stability of CaM$_{boundary}$. The 4-fold drop in binding to smMLCK caused by E127Q in the CaM$_{boundary}$ background was consistent with the disruption of an intermolecular salt bridge to an Arg on smMLCK.

Unlike CaM$_{boundary}$, both molecules predicted by the modified methods, CaMmod$_{boundary}^{no\_bias}$ and CaMmod$_{boundary}^{bias}$, retained tight binding to smMCLK. These results support the use of a stronger electrostatic potential and a larger rotamer library in the CaM–smMLCK optimization. Introducing bias into the energy function to obtain CaMmod$_{boundary}^{bias}$ resulted in a 3-fold improvement in K_d relative to CaMmod$_{boundary}^{no\_bias}$ (Table 1). At the sequence level, CaMmod$_{boundary}^{no\_bias}$ and CaMmod$_{boundary}^{bias}$ differ only at position 123, where a wild-type glutamate is substituted by a lysine in CaMmod$_{boundary}^{no\_bias}$ and a glutamine in CaMmod$_{boundary}^{bias}$. Lys-123 in CaMmod$_{boundary}^{no\_bias}$ could reduce binding to smMLCK by forming favorable intramolecular electrostatic interactions with neighboring glutamates (Glu-120 or Glu-127), at the expense of forming unfavorable intermolecular electrostatic interactions with the positively charged target peptide.

These results support previous findings on the importance of glutamates for the target recognition mechanism of CaM (11, 12, 17). CaM$_{wt}$ is able to bind tightly to a variety of targets by using a subset of available glutamates in salt-bridge interactions. Removal of a single intermolecular salt bridge between CaM and smMLCK produces a 3- to 4-fold reduction in CaM's binding to the target.
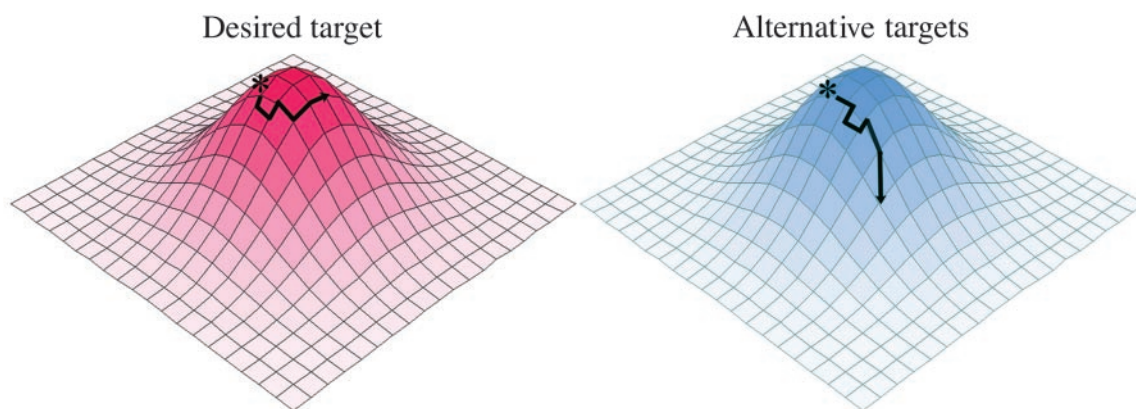

Fig. 3. Fitness of CaM interacting with the desired target, smMLCK (red), and with alternative targets (blue). The CaM$_{wt}$ sequence lies near the respective maxima for both the desired target and the alternative targets as indicated by *. Arrows show the change in fitness due to mutations in the CaM sequence predicted by the optimization.

Table 3. Energies of WT and redesigned CaM–target complexes*

	smMLCK	skMLCK	CaMKI	CaMKII[†]	CaMKK
CaM$_{wt}$	−579.4	−510.5	−704.8	−612.0	−748.4
CaM$_{core}$	−621.3	−494.3	>1,000[‡]	−478.2	−731.7
CaMmod$_{boundary}^{bias}$	−649.4	−481.8	>1,000[‡]	−472.5	−706.3

*The energies of CaM$_{wt}$ and the redesigned CaM variants were calculated in context of the available structures for CaM–target complexes by using the set of positions shown in Table 1. All calculations were carried out by using no biasing of the energy function, the larger rotamer library, a dielectric constant of 4r, and the Dead-End Elimination theorem (28, 29).

[†]CaM residues 74–83 are missing from the crystal structure of the CaM–CaMKII complex and, hence, were omitted from the calculations.

[‡]The large energy is due to a van der Waals clash between Tyr-84 on CaM and Ala-154 on CaMKI, which results from the fixed backbone approximation used in the calculations.

Positive vs. Negative Design in Improving CaM-Binding Specificity. In the present work, we were able to increase the binding specificity of CaM by optimizing its interactions with the desired target, smMLCK. However, the increase in binding specificity was not due to CaM's improved binding affinity to smMLCK but due to its decreased binding affinity to the alternative targets. Considering that the alternative targets were not included in the optimization procedure, the results seem counterintuitive.

CaM has evolved to bind tightly to a large number of targets. The fitness of CaM$_{wt}$ is nearly optimal with respect to its sequence for all CaM targets. Fig. 3 illustrates the change in fitness of CaM for interactions with its targets during the computational optimization procedure. The two surfaces represent the fitness of CaM interacting with the desired target, smMLCK, and with alternative targets. The computational optimization of the CaM–smMLCK complex results in sequence changes that improve or maintain CaM's ability to bind smMLCK (Fig. 3). Because no information from the alternative targets is included in the optimization procedure, the sequence changes are essentially random with respect to interactions with the latter targets. Given that the fitness of CaM$_{wt}$ is near optimal for each CaM-target complex, the probability of increasing fitness by a random sequence change is very low. Hence, without directly including negative design in the calculations, we expect to obtain CaM sequences that on average show decreased binding affinities to the alternative targets, and thus increased binding specificity for the desired target. Energies calculated for CaM$_{wt}$, CaM$_{core}$, and CaMmod$_{boundary}^{bias}$ in the context of five available CaM-target complex structures (10–12, 15, 17) support this argument (Table 3). As expected, the energy of the CaM–smMLCK complex is decreased (improved) by changing the sequence from CaM$_{wt}$ to CaM$_{core}$ to CaMmod$_{boundary}^{bias}$. For the alternative targets, the opposite trend is evident: the energies of the CaM–target complexes are most favorable for the CaM$_{wt}$ sequence, less favorable for the CaM$_{core}$ sequence, and least favorable for the CaMmod$_{boundary}^{bias}$ sequence.

The further we move away from the CaM$_{wt}$ sequence, while improving or preserving the fitness of interaction with the desired target, the more specificity we achieve. This argument suggests that simultaneously optimizing a larger number of CaM positions would increase the chances of obtaining a protein with increased binding specificity. This finding is indeed confirmed by the experimental results: the binding specificity of CaMmod$_{boundary}^{bias}$, which included additional boundary and surface positions, was greater than that of the core design, CaM$_{core}$. Expanding the number of optimization positions could increase CaM-binding specificity either through the cumulative effect of multiple, slightly improved interactions or through the effect of a small number of critical interactions. Although the proposed model (Fig. 3) accommodates both possibilities, the current data do not allow us to discriminate between these two extremes. It is likely, however, that both mechanisms operate to different extents for different targets.

In recent work on binding specificity design in coiled coils, Havranek and Harbury (39) showed that both positive and negative design are necessary to achieve binding specificity for coiled-coil homodimers and heterodimers. The present work shows that, in the case of CaM, optimizing its interactions with only the desired target could be sufficient. Because CaM has a significantly more complex architecture compared with a coiled coil, it has a greater number of potential interactions to favor one target over another. Nevertheless, incorporating negative design in the optimization of the CaM–target interface is likely to improve the chances of obtaining increased binding specificity. Direct incorporation of negative design would ensure that the optimization procedure generates CaM variants with improved or maintained fitness for the interaction with the desired target, while simultaneously decreasing fitness for interactions with the alternative targets.

1. Weinstein, H. & Mehler, E. L. (1994) *Annu. Rev. Physiol.* **56,** 213–236.
2. Crivici, A. & Ikura, M. (1995) *Annu. Rev. Biophys. Biomol. Struct.* **24,** 85–116.
3. Zielinski, R. E. (1998) *Annu. Rev. Plant Physiol. Plant Mol. Biol.* **49,** 697–725.
4. O'Neil, K. T. & DeGrado, W. F. (1990) *Trends Biochem. Sci.* **15,** 59–64.
5. Chin, D. & Means, A. R. (2000) *Trends Cell Biol.* **10,** 322–328.
6. Wintrode, P. L. & Privalov, P. L. (1997) *J. Mol. Biol.* **266,** 1050–1062.
7. Brokx, R. D., Lopez, M. M., Vogel, H. J. & Makhatadze, G. I. (2001) *J. Biol. Chem.* **276,** 14083–14091.
8. Gomes, A. V., Barnes, J. A. & Vogel, H. J. (2000) *Arch. Biochem. Biophys.* **379,** 28–36.
9. Moorthy, A. K., Gopal, B., Bhattacharya, S., Bhattacharya, A., Murthy, M. R. N. & Surolia, A. (1999) *FEBS Lett.* **461,** 19–24.
10. Ikura, M., Clore, G. M., Gronenborn, A. M., Guang, Z., Klee, C. B. & Bax, A. (1992) *Science* **256,** 632–638.
11. Meador, W. E., Means, A. R. & Quiocho, F. A. (1992) *Science* **257,** 1251–1255.
12. Meador, W. E., Means, A. R. & Quiocho, F. A. (1993) *Science* **262,** 1718–1721.
13. Elshorst, B., Hennig, M., Forsterling, H., Diener, A., Maurer, M., Schulte, P., Schwalbe, H., Griesinger, C., Krebs, J., Schmid, H., *et al.* (1999) *Biochemistry* **38,** 12320–12332.
14. Osawa, M., Swindells, M. B., Tanikawa, J., Tanaka, T., Mase, T., Furuya, T. & Ikura, M. (1998) *J. Mol. Biol.* **276,** 165–176.
15. Osawa, M., Tokumitsu, H., Swindells, M. B., Kurihara, H., Orita, M., Shibanuma, T., Furuya, T. & Ikura, M. (1999) *Nat. Struct. Biol.* **6,** 819–824.
16. Schumacher, M. A., Rivard, A. F., Bachinger, H. P. & Adelman, J. P. (2001) *Nature* **410,** 1120–1124.
17. Kurokawa, H., Osawa, M., Kurihara, H., Katayama, N., Tokumitsu, H., Swindells, M. B., Kainosho, M. & Ikura, M. (2001) *J. Mol. Biol.* **312,** 59–68.
18. Erickson-Viitanen, S. & DeGrado, W. F. (1987) *Methods Enzymol.* **139,** 455–478.
19. Dahiyat, B. I. & Mayo, S. L. (1997) *Science* **278,** 82–87.
20. Malakauskas, S. M. & Mayo, S. L. (1998) *Nat. Struct. Biol.* **5,** 470–475.
21. Shimaoka, M., Shifman, J. M., Jing, H., Takagi, J., Mayo, S. L. & Springer, T. A. (2000) *Nat. Struct. Biol.* **7,** 674–678.
22. Bolon, D. N. & Mayo, S. L. (2001) *Proc. Natl. Acad. Sci. USA* **98,** 14274–14279.
23. Marshall, S. A. & Mayo, S. L. (2001) *J. Mol. Biol.* **305,** 619–631.
24. Shifman, J. M. & Mayo, S. L. (2002) *J. Mol. Biol.* **323,** 417–423.
25. Street, A. G. & Mayo, S. L. (1999) *Struct. Fold. Des.* **5,** R105–R109.
26. Dunbrack, R. L. & Karplus, M. (1993) *J. Mol. Biol.* **230,** 543–574.
27. Gordon, D. B., Marshall, S. A. & Mayo, S. L. (1999) *Curr. Opin. Struct. Biol.* **9,** 509–513.

28. Desmet, J., De Maeyer, M., Hazes, B. & Lasters, I. (1992) *Nature* **356,** 539–542.
29. Gordon, D. B., Hom, G. K., Mayo, S. L. & Pierce, N. A. (2003) *J. Comp. Chem.* **24,** 232–243.
30. Kirckpatrick, S., Gelatt, C. D. & Vecchi, M. P. (1983) *Science* **220,** 671–680.
31. Voight, C. A., Gordon, D. B. & Mayo, S. L. (2000) *J. Mol. Biol.* **299,** 789–803.
32. Prodromou, C. & Pearl, L. H. (1992) *Protein Eng.* **5,** 827–829.
33. O'Neil, K. T., Wolfe, H. R., Erickson-Viitanen, S. & DeGrado, W. F. (1987) *Science* **236,** 1454–1456.
34. Papoian, G. A., Ulander, J. & Wolynes, P. G. (2003) *J. Am. Chem. Soc.* **125,** 9170–9178.
35. Street, A. G., Datta, D., Gordon, D. B. & Mayo, S. L. (2000) *Phys. Rev. Lett.* **84,** 5010–5013.
36. Xu, D., Lin, S. L. & Nussinov, R. (1997) *J. Mol. Biol.* **265,** 68–84.
37. Hendsch, Z. S. & Tidor, B. (1999) *Protein Sci.* **8,** 1381–1392.
38. Lee, L.-P. & Tidor, B. (2001) *Protein Sci.* **10,** 362–377.
39. Havranek, J. J. & Harbury, P. B. (2003) *Nat. Struct. Biol.* **10,** 45–52.
40. Koradi, R., Billeter, M. & Wüthrich, K. (1996) *J. Mol. Graphics* **14,** 51–55.

BIOPHYSICS

Table 4. Computational details and binding of CaM variants to smMLCK

Sequence names as reported in main text	Computational parameters*	11	12	14	18	55	76	83	84	87	91	109	114	116	120	123	127	145	K_d, nM
CaM$_{wt}$	$\varepsilon = 40r$ srl No bias	E	F	E	L	V	M	E	E	E	V	M	E	L	E	E	E	M	1.8 ± 1.3
CaM$_{core}$	$\varepsilon = 40r$ srl No bias	L	Y	-	-	I	E	-	Y	-	I	L	-	-	-	-	-	I	1.3 ± 0.9
CaM$_{boundary}$	$\varepsilon = 40r$ srl No bias	L	Y	D	-	I	E	R	Y	L	I	L	I	E	-	-	Q	I	114 ± 83[‡]
	$\varepsilon = 4r$ srl No bias	L	Y	-	-	I	E	K	Y	K	I	L	I	E	-	K	D	I	28 ± 6
	$\varepsilon = 4r$ srl Bias	L	Y	D	E	I	E	K	Y	L	I	L	I	E	-	Q	E	I	≈1,000[‡]
	$\varepsilon = 40r$ lrl No bias	L	Y	-	-	I	E	K	Y	L	I	L	I	E	K	-	K	I	≈1,000[‡]
	$\varepsilon = 40r$ lrl Bias	L	Y	-	-	I	E	N	Y	K	I	L	I	E	D	Q	-	I	20 ± 3
	$\varepsilon = 4r$ lrl No bias	L	Y	-	-	I	E	R	Y	K	I	L	I	E	-	K	-	I	6.1 ± 0.8
	$\varepsilon = 4r$ lrl Bias	L	Y	-	-	I	E	R	Y	K	I	L	I	E	-	Q	-	I	2.3 ± 0.7

*CaM optimizations were performed with different dielectric constants ($\varepsilon = 40r$ or $4r$), different rotamer libraries [standard rotamer library (srl), or large rotamer library (lrl)], and different energy functions [standard (no bias) or modified to enhance intermolecular interactions (bias)].

[†]Eight boundary and surface positions in the CaM–smMLCK binding interface were optimized. Position 18 was also included in two calculations that used the dielectric constant of $4r$ and the standard rotamer library. Dashes indicate sequence identity to CaM$_{wt}$. Eight core mutations, highlighted in gray, were carried over from CaM$_{core}$.

[‡]The majority of loss in binding affinity to smMLCK for these CaM variants was attributed to a single mutation, E87L.